

On the violation of the Fermi-liquid picture in two-dimensional systems owing to the Van-Hove singularities

V.Yu.Irkhin* and A.A.Katanin

Institute of Metal Physics, 620219 Ekaterinburg, Russia

Abstract

We consider the two-dimensional t - t' Hubbard model with the Fermi level being close to the Van-Hove singularities. The phase diagram of the model is discussed. Far from the quantum phase transition (QPT) into ferro- (antiferro-) magnetic state, the self-energy at the singularity points has a nearly-linear energy dependence, the density of states being proportional to $\ln^3 |\varepsilon|$. In the quantum-disordered and quantum-critical regime near QPT a scaling approach is used. At small energies the self-energy demonstrates a power-like behavior with the exponent changing from unity to zero in a narrow energy interval. Provided that the system is close to ferromagnetic instability which occurs at $t'/t \rightarrow -1/2$, the quasiparticle spectral weight has, instead of a narrow peak, a broad maximum and is non-monotonous at small energies. The application of the results to cuprates is discussed.

I. INTRODUCTION

Last decade, a possibility of a non-Fermi-liquid (NFL) behavior in two-dimensional (2D) systems has been a subject of many theoretical investigations. This question is especially interesting in connection with the high-temperature superconductors where many unconventional features, including pseudogap phenomena, are observed. Anderson [1] has put forward the idea that a 2D system can demonstrate NFL behavior at arbitrary small interelectron repulsion U owing to a finite phase shift at the Fermi energy. Even in the absence of such effects, a NFL state can occur at small U because of peculiarities of electron or spin and charge fluctuation spectra.

In the usual 2D Fermi liquid the imaginary part of the self-energy (electron damping) has the energy dependence $\text{Im}\Sigma(\mathbf{k}_F, \varepsilon) \propto \varepsilon^2 \ln |\varepsilon|$ [2,3], and the temperature behavior of resistivity is $\rho \propto T^2 \ln T$ [4]. However, these dependences do not describe experimental data on high- T_c cooper-oxide compounds. To treat the anomalous behavior of these systems, Varma et al [5] proposed the phenomenological marginal Fermi-liquid (MFL) theory where $\text{Im}\Sigma(\mathbf{k}_F, \varepsilon) \propto |\varepsilon|$. Then the electronic specific heat should demonstrate $T \ln T$ -dependence, and the resistivity the T -linear behavior. A similar behavior in a broad temperature region can be obtained in the presence of strong antiferromagnetic fluctuations for 2D and nested 3D systems [6,7].

The anomalous electron properties of 2D lattice systems can be explained by the presence of the Van-Hove (VH) singularities [8]. In the presence of these singularities, the bare electron density of states is logarithmically divergent. Provided that the Fermi level lies close to the VH peak, we can restrict ourselves to considering only close vicinity of the VH points of spectrum when treating electron properties. As discussed in detail in Ref. [9], an interplay of superconducting, antiferro- and ferromagnetic channels takes place in this case. This leads to quantum phase transitions into the corresponding ordered states as band filling approaches the VH one. Recently, these results were confirmed by a temperature-dependent RG approach [10], which takes into account the contribution from the whole Fermi surface.

In the presence of VH singularities we have to leading (second) order in U the behavior $\text{Im}\Sigma(\mathbf{k}_F, \varepsilon) \propto |\varepsilon| \ln|1/\varepsilon|$ (\mathbf{k}_F is assumed to be VH point), which differs slightly from the linear dependence in the MFL theory. However, an important question occurs how this behavior changes with taking into account higher-order terms. This problem was discussed in Refs. [11,12]. The conclusions of different approaches turned out to be contradictory: a possibility of a NFL state is discussed in Ref. [11], while a standard Fermi-liquid behavior was found in Ref. [12]. It should be noted that in both the papers only part of all the possible interaction channels was taken into account. However, as it was demonstrated in Ref. [9], all the scattering channels are equally important, which can substantially change the previous results.

In the present paper we consider the energy-dependence of the self-energy with account of all the scattering channels. We demonstrate that a violation of the Fermi-liquid picture takes place provided that the system is close to quantum phase transition into a magnetically ordered or superconducting state. Our approach can be considered as a generalization of that of Ref. [13] to the case of a non-nested Fermi surface. The results for nearly antiferromagnetic state are similar to those obtained in Refs. [14] with account of the contribution of whole Fermi-surface. We consider also nearly ferromagnetic state where effects of violation of Fermi-liquid behavior are stronger. The behavior of some physical properties and application of the results obtained to cuprates is discussed in the Conclusion.

II. THE MODEL AND VAN-HOVE SINGULARITIES

We consider the t - t' Hubbard model on the square lattice:

$$H = \sum_{\mathbf{k}} \varepsilon_{\mathbf{k}} c_{\mathbf{k}\sigma}^\dagger c_{\mathbf{k}\sigma} + U \sum_i n_{i\uparrow} n_{i\downarrow} \quad (1)$$

with the electron spectrum

$$\varepsilon_{\mathbf{k}} = -2t(\cos k_x + \cos k_y) - 4t' \cos k_x \cos k_y + 4t' - \mu \quad (2)$$

Hereafter we assume $t > 0$, $t' < 0$ (which is the case for hole-doped systems), $0 \leq |t'/t| < 1/2$. We have picked out the term $4t'$ for further convenience. For $t' = 0$ the Fermi surface is nested, which results in peculiarities of physical properties [13,7]. However, nesting is removed for $t'/t \neq 0$. For arbitrary t'/t , the spectrum (2) contains VH singularities connected with the points $A = (\pi, 0)$, $B = (0, \pi)$. The chemical potential μ is determined by the electron concentration n and can be obtained from the condition

$$n = \sum_{\mathbf{k}} f_{\mathbf{k}} \quad (3)$$

with $f_{\mathbf{k}} = f(\varepsilon_{\mathbf{k}})$ being the Fermi function, so that $\mu = 0$ corresponds to Van Hove filling. Being expanded near the VH singularity points, the spectrum (2) takes the form

$$\varepsilon_{\mathbf{k}}^A = -2t(\sin^2 \varphi \bar{k}_x^2 - \cos^2 \varphi k_y^2) = -2t k_+ k_- - \mu \quad (4a)$$

$$\varepsilon_{\mathbf{k}}^B = 2t(\cos^2 \varphi k_x^2 - \sin^2 \varphi \bar{k}_y^2) = 2t \tilde{k}_+ \tilde{k}_- - \mu \quad (4b)$$

where

$$\begin{aligned} k_{\pm} &= \sin \varphi \bar{k}_x \pm \cos \varphi k_y \\ \tilde{k}_{\pm} &= \cos \varphi k_x \pm \sin \varphi \bar{k}_y \end{aligned} \quad (5)$$

$\bar{k}_x = \pi - k_x$, $\bar{k}_y = \pi - k_y$, φ is the half of the angle between asymptotes at VH singularity, $2\varphi = \cos^{-1}(-2t'/t)$.

III. QUANTUM PHASE TRANSITIONS

We have a set of quantum phase transitions (QPT's) for the model (1), see Ref. [9]. We restrict ourselves to the case of small enough $U \lesssim 8t$, so that we may neglect the correlation effects connected with Hubbard's subband formation (e.g., the Mott-Hubbard metal-insulator transition). Provided that the electron concentration is not too close to its Van Hove value, i.e. the chemical potential satisfies $|\mu| > \mu_c$, μ_c being the critical value, we have the normal (paramagnetic and non-superconducting) phase. When approaching the

VH singularity, a QPT to antiferromagnetic, superconducting or ferromagnetic state occurs. The type of the ground state depends on t'/t and U . In particular, for $U = 4t$ we have the antiferromagnetic ground state at $|t'/t| < 0.30$ and ferromagnetic one for larger $|t'/t|$ [9]. The critical electron concentrations for stability of these phases differ by several percents from Van-Hove filling.

In the vicinity of QPT we have, as follows from general considerations [15,16], three temperature regions (Fig.1). At $|\mu| > \mu_c$ (disordered ground state) and $T \ll |\mu| - \mu_c$ we have the quantum-disordered (QD) regime where the correlation length $\xi_{cr}(T)$ deviates from the ground-state value by exponentially small corrections only. For the ordered ground state ($|\mu| < \mu_c$) we have at $T \ll \mu_c - |\mu|$ the renormalized classical (RC) regime with exponentially large correlation length. Finally, at $T \gg |\mu_c - |\mu||$ we have the quantum-critical (QC) regime with a power temperature dependence of the correlation length.

Further we treat the QD and QC regimes. The region $|\mu| < \mu_c$, $T < T_c$, where strong short-range order takes place, cannot be considered by the renormalization-group approach which starts from a non-magnetic (non-superconducting) Fermi-liquid state.

IV. ELECTRON SELF-ENERGY IN THE SECOND ORDER

Consider first zero-temperature perturbative results. To second order the expression for the electron self-energy has the form

$$\Sigma^{(2)}(\mathbf{k}, \varepsilon) = U^2 \sum_{\mathbf{p}, \mathbf{q}} \frac{f_{\mathbf{p}+\mathbf{q}-\mathbf{k}}(1 - f_{\mathbf{p}} - f_{\mathbf{q}}) + f_{\mathbf{p}} f_{\mathbf{q}}}{\varepsilon + \varepsilon_{\mathbf{p}+\mathbf{q}-\mathbf{k}} - \varepsilon_{\mathbf{p}} - \varepsilon_{\mathbf{q}}} \quad (6)$$

This contribution can be represented as a sum of three diagrams (Fig.2 a-c):

$$\Sigma^{(2)}(\mathbf{k}, \varepsilon) = \Sigma_1(\mathbf{k}, \varepsilon) + \Sigma_2(\mathbf{k}, \varepsilon) + \Sigma_3(\mathbf{k}, \varepsilon) \quad (7)$$

When picking out the singularities we can put $\varepsilon_{\mathbf{p}} = \varepsilon_{\mathbf{p}}^A$ or $\varepsilon_{\mathbf{p}} = \varepsilon_{\mathbf{p}}^B$ for \mathbf{p} being close to $A(B)$ Van-Hove points. Note that the term Σ_1 was investigated earlier [11,12,17]. We restrict our consideration to the VH points at the Fermi surface, $\mathbf{k}_F = (0, \pi)$ or $(\pi, 0)$. The calculations yield:

$$\begin{aligned} \text{Re}\Sigma_1(\mathbf{k}_F, \varepsilon) &= -(\ln 2)(g_0/\sin 2\varphi)^2 \varepsilon \ln^2(\Lambda^2|t/\varepsilon|) \\ \text{Re}\Sigma_{2,3}(\mathbf{k}_F, \varepsilon) &= -(g_0/\sin 2\varphi)^2 \varepsilon \begin{cases} A_{2,3} \ln(\Lambda^2|t/\varepsilon|) & |\varepsilon/t| \ll \cos 2\varphi \\ k_{2,3} \ln 2 \ln^2(\Lambda^2|t/\varepsilon|) & |\varepsilon/t| \gg \cos 2\varphi \end{cases} \end{aligned} \quad (8)$$

where $g_0 = U/(4\pi^2 t)$ is the dimensionless coupling constant, $\Lambda \sim 1$ is the ultraviolet momentum cutoff, $k_2 = 1$, $k_3 = 2/3$,

$$\begin{aligned} A_2 &= \int_0^{\cos 2\varphi} \frac{dx}{x} \ln \frac{\varepsilon_x - x}{\varepsilon_x} + \frac{1}{2} \int_{\cos 2\varphi}^{1/\cos 2\varphi} \frac{dx}{x} \ln \frac{\varepsilon_x + x}{\varepsilon_x} \\ &\quad + \frac{1}{2} \int_{-\infty}^0 \frac{dx}{x} \ln \frac{\varepsilon_x}{\varepsilon_x + x} \end{aligned} \quad (9a)$$

$$\begin{aligned} A_3 &= \int_0^{\cos 2\varphi} \frac{dx}{2\varepsilon_x + x} \ln \left(-\frac{x}{2\varepsilon_x} \right) + \frac{1}{2} \int_{\cos 2\varphi}^{1/\cos 2\varphi} \frac{dx}{2\varepsilon_x + x} \ln \frac{2(\varepsilon_x + x)}{x} \\ &\quad + \frac{1}{2} \int_{-\infty}^0 \frac{dx}{2\varepsilon_x + x} \ln \frac{x}{2(\varepsilon_x + x)} \end{aligned} \quad (9b)$$

with $\varepsilon_x = (x - \cos 2\varphi)(1 - x \cos 2\varphi)/\sin^2 2\varphi$. For small energies $|\varepsilon| \ll |\mu|$ the real part remains linear in energy with the difference that logarithmical divergences are cut at $|\mu|$ rather than at $|\varepsilon|$. The corresponding imaginary parts at $|\varepsilon| \gg |\mu|$ read

$$\begin{aligned} \text{Im}\Sigma_1(\mathbf{k}_F, \varepsilon) &= -(\pi \ln 2)(g_0/\sin 2\varphi)^2 |\varepsilon| \ln(\Lambda^2|t/\varepsilon|) \\ \text{Im}\Sigma_{2,3}(\mathbf{k}_F, \varepsilon) &= -\pi(g_0/\sin 2\varphi)^2 |\varepsilon| \begin{cases} B_{2,3} & |\varepsilon/t| \ll \cos 2\varphi \\ k_{2,3} \ln 2 \ln(\Lambda^2|t/\varepsilon|) & |\varepsilon/t| \gg \cos 2\varphi \end{cases} \end{aligned} \quad (10)$$

where

$$B_2 = (A_{21} + A_{23})\theta(\varepsilon) + A_{22}\theta(-\varepsilon)$$

$$B_3 = (A_{31} + A_{33})\theta(-\varepsilon) + A_{32}\theta(\varepsilon)$$

and A_{2n} and A_{3n} are n -th summands in the definition of A_2 and A_3 , Eq. (9), respectively, $\theta(\varepsilon)$ is the step function. At $t'/t \neq 0$ we have $\text{Im}\Sigma(\mathbf{k}_F, \varepsilon) \neq \text{Im}\Sigma(\mathbf{k}_F, -\varepsilon)$ because of the absence of the particle-hole symmetry for the less singular terms $\Sigma_{2,3}(\mathbf{k}_F, \varepsilon)$. This fact results in an

asymmetry of the electron density of states near the Fermi level and can be important for some physical properties, e.g., thermoelectric power. Unlike the real part of the self-energy, the imaginary part changes its dependence to quadratic one at $|\varepsilon| \ll |\mu|$ demonstrating a conventional Fermi-liquid behavior in this region. The corresponding coefficient at ε^2 can be obtained from the real part via Kramers-Kronig relations.

V. RENORMALIZATION

Both real and imaginary parts of the self-energy contain large logarithms at $|\mu| \ll |\varepsilon| \ll t$. Therefore we can introduce the logarithmic variable $\xi = \ln(\Lambda|t/\varepsilon|^{1/2})$. Then the leading terms of the expansion in the powers of interaction strength can be written down as

$$\Sigma(\xi) = A g_0^2 \xi (1 + C_1 g_0 \xi + D_1 g_0 \xi^2 + \dots)$$

To perform the summation of leading logarithms in the self-energy, we introduce the vertices $\gamma_i(\xi)$, $i = 1, \dots, 4$ (Fig. 2), and consider the renormalization of Σ . As discussed in Refs. [18,19,9], $\gamma_i(\xi)$ can be determined from the renormalization-group (RG) equations

$$\begin{aligned} \gamma'_1 &= 2d_1(\xi)\gamma_1(\gamma_2 - \gamma_1) + 2d_2\gamma_1\gamma_4 - 2d_3\gamma_1\gamma_2 \\ \gamma'_2 &= d_1(\xi)(\gamma_2^2 + \gamma_3^2) + 2d_2(\gamma_1 - \gamma_2)\gamma_4 - d_3(\gamma_1^2 + \gamma_2^2) \\ \gamma'_3 &= -2d_0(\xi)\gamma_3\gamma_4 + 2d_1(\xi)\gamma_3(2\gamma_2 - \gamma_1) \\ \gamma'_4 &= -d_0(\xi)(\gamma_3^2 + \gamma_4^2) + d_2(\gamma_1^2 + 2\gamma_1\gamma_2 - 2\gamma_2^2 + \gamma_4^2) \end{aligned} \quad (11)$$

where $\gamma'_i \equiv d\gamma_i/d\xi$,

$$\begin{aligned} d_0(\xi) &= 2c_0\xi; \\ d_1(\xi) &= 2 \begin{cases} \xi, & \xi < 2z_{\mathbf{Q}} \\ z_{\mathbf{Q}}, & \xi > 2z_{\mathbf{Q}} \end{cases} \\ d_2 &= 2z_0; \quad d_3 = 2c_{\mathbf{Q}} \end{aligned} \quad (12)$$

The quantities

$$z_0 = c_0 = 1/\sin(2\varphi) = 1/\sqrt{1-R^2}$$

are the prelogarithmic factors in small-momentum particle-hole and particle-particle bubble, while

$$\begin{aligned} z_{\mathbf{Q}} &= \ln[(1 + \sqrt{1 - R^2})/R] \\ c_{\mathbf{Q}} &= \tan^{-1}(R/\sqrt{1 - R^2})/R \end{aligned} \quad (13)$$

are the prelogarithmic factors in particle-hole and particle-particle bubble with momenta close to $\mathbf{Q} = (\pi, \pi)$, $R = -2t'/t$. Equations (11) should be solved with the initial condition $\gamma_i(0) = g_0$. The magnetic or superconducting instabilities manifest in the divergence of the corresponding quantity $\gamma_i(\xi)$ at some critical scale ξ_c . This is connected with the critical energy scales discussed in Sect. II as $\mu_c \sim T_c \sim \Lambda \exp(-2\xi_c)$, for a detailed discussion see Ref. [9]. In the absence of interlayer coupling the quantity T_c has the meaning of a temperature of crossover into the state with pronounced short-range order (or pseudogap state) rather than of a phase transition temperature. In fact, T_c determines the border between the quantum-critical regime and quantum-disordered or renormalized classical regime.

For the quantum-disordered regime (which can be roughly identified as $T \ll |\mu|$) we should stop scaling at

$$\xi^* = \ln[\Lambda t^{1/2} / \max(|\mu|, |\varepsilon|)^{1/2}] \quad (\text{QD}) \quad (14)$$

while for quantum-critical regime ($T \gg |\mu|$) at

$$\xi^* = \ln[\Lambda t^{1/2} / \max(T, |\varepsilon|)^{1/2}] \quad (\text{QC}) \quad (15)$$

The condition $|\mu| > \mu_c$ or $T > T_c$ guarantees that the system is outside the renormalized-classical regime and $\xi^* < \xi_c$.

Because of the presence of double-logarithmic terms, the corresponding RG equations are only approximate. However, the comparison of the results of their solution [9] with the RG approach which takes into account the whole Fermi-surface [10] shows that they reproduce well the renormalization of the couplings.

Now we consider the renormalization of the self-energy. We follow the method of Refs. [20–22]. Defining the scale-dependent quasiparticle residue

$$Z(\xi) = Z_1(\xi)Z_2(\xi)Z_3(\xi)$$

where Z_i ($i = 1, 2, 3$) is the contribution of i -th diagram, we have the RG equations

$$\begin{aligned} \frac{d \ln Z_1(\xi)}{d \xi} &= -(4 \ln 2) \xi \gamma_4^2 / \sin^2 2\varphi \\ \frac{d \ln Z_2(\xi)}{d \xi} &= -D_2(\xi)(\gamma_1^2 + \gamma_2^2 - \gamma_1 \gamma_2) / \sin^2 2\varphi \\ \frac{d \ln Z_3(\xi)}{d \xi} &= -D_3(\xi) \gamma_3^2 / \sin^2 2\varphi \end{aligned} \quad (16)$$

Here

$$D_{2,3}(\xi) = \begin{cases} 4k_{2,3}\xi \ln 2 & \xi < (1/2) \ln(1/\cos 2\varphi) \\ A_{2,3} & \xi > (1/2) \ln(1/\cos 2\varphi) \end{cases}$$

and the summation over spin indices in vertices is performed. Then the real part of the self-energy can be found as

$$\text{Re}\Sigma(\mathbf{k}_F, \varepsilon) = \varepsilon \ln Z(\xi^*) \quad (17)$$

(see, e.g., Ref. [22]). After calculating $\text{Re}\Sigma$, the imaginary part of the self-energy can be obtained from the Kramers-Kronig relations.

VI. RESULTS OF CALCULATIONS

First, we demonstrate our approach in a simple case with the only non-zero vertex, $\gamma_4 \neq 0$. As discussed in Ref. [9], this case corresponds to $t' \rightarrow -t/2$, the ground state at Van-Hove filling being ferromagnetic (flat-band ferromagnetism). Then we have

$$\gamma_4 = \frac{g_0}{1 + g_0(c_0 \xi^2 - 2z_0 \xi)} \quad (18)$$

The vertex (18) diverges in the critical point

$$\xi_c = \frac{1}{2} \ln \frac{\Lambda^2 t}{\max(\mu, T)} = 1 - \sqrt{1 - 1/(z_0 g_0)} \quad (19)$$

where we have put $z_0 = c_0$ in ξ_c according to (13). From (16) we obtain $Z_2 = Z_3 = 1$ and

$$Z_1 = \exp \left[-\frac{4 \ln 2}{\sin^2 2\varphi} \frac{g_0^2 \xi (\xi - 1)}{(1 - g_0 z_0)(1 + g_0 z_0 \xi^2 - 2 g_0 z_0 \xi)} \right] \quad (20)$$

For ξ being close to ξ_c we have

$$\gamma_4 \sim \xi_{cr}^2(T = 0) \sim (\xi_c - \xi)^{-1} \quad (21)$$

As well as in the nesting case (see, e.g., Ref. [13]), the quasiparticle weight Z vanishes exponentially in the QPT point. Note that this vanishing is much faster than the inverse-logarithmic dependence

$$Z \sim \frac{1}{\ln^q(\xi_c - \xi)}, \quad q \simeq 0.35 \quad (22)$$

obtained in Ref. [11] where only one scattering channel was taken into account. Besides nearly-linear dependences in ε (with logarithmic corrections), both real and imaginary part of the self-energy contain large ε -dependent factors of the order of $1/(\xi_c - \xi)^2 \propto \xi_{cr}^4(0)$, which occur because of the divergence of the vertex (18) at $\xi \rightarrow \xi_c$.

As discussed in Ref. [9], for $|t'/t|$ being far from $1/2$ we have an interplay of all the scattering channels, so that we have to solve Eqs. (11), (16) numerically. We also calculate the quasiparticle spectral weight in VH points of the Fermi surface,

$$A(\mathbf{k}_F, \varepsilon) = -\frac{1}{\pi} \frac{\text{Im}\Sigma(\mathbf{k}_F, \varepsilon)}{[\varepsilon - \text{Re}\Sigma(\mathbf{k}_F, \varepsilon)]^2 + [\text{Im}\Sigma(\mathbf{k}_F, \varepsilon)]^2} \quad (23)$$

The results of the calculations for $t' = -0.15t$, $\mu/t = 2 \cdot 10^{-4}$, $T = 0$ (nearly antiferromagnetic ground state, $\mu_c/t = 10^{-4}$) and for $t' = -0.45t$, $\mu/t = 0.045$, $T = 0$ (nearly ferromagnetic ground state, $\mu_c/t = 0.04$) are shown in Figs. 3,4. One can see that renormalization of the second-order result is rather strong. In both the cases the self-energy demonstrates a power-like behavior at small energies with the effective exponent

$$\alpha(\varepsilon) = \frac{\partial \ln |\text{Re}\Sigma(\mathbf{k}_F, \varepsilon)|}{\partial \ln \varepsilon} \quad (24)$$

varying from unity to zero in a narrow energy region. While at $t'/t = -0.15$ we have a well-defined peak in the quasiparticle weight, at $t' = -0.45t$ the peak is broadened and a non-monotonous dependence occurs at small energies. Both the peak in $\text{Re}\Sigma(\mathbf{k}_F, \varepsilon)$ and non-monotonous dependence of $A(\mathbf{k}_F, \varepsilon)$ occur at the scales of the order of μ . The imaginary part of the self-energy becomes large enough in the nearly-ferromagnetic case. The reason of the difference between the nearly antiferro- and ferromagnetic states is the factor of $1/\sin^2 2\varphi$ in Eq.(16), which is large for $|t'/t|$ being close to $1/2$. Besides that, the critical energy scale μ_c in the antiferromagnetic case is very small. One can expect that including the contribution of the Fermi surface flat regions, which are important at small enough $|t'/t|$, will increase the tendency toward antiferromagnetism (see, e.g., Refs. [10,23]). Therefore the self-energy behavior will be similar to that in ferromagnetic case.

With increasing the chemical potential (so that the system is moved away from QPT), the higher-order renormalizations become less important. This is demonstrated in Fig. 5 for the case of intermediate values $t' = -0.3t$, where two-patch approach gives a very small critical chemical potential, $\ln(t/\mu_c) \simeq 362$. We have a nearly linear energy dependence of $\text{Im}\Sigma(\mathbf{k}_F, \varepsilon)$ in a broad energy region (except for very small energies $|\varepsilon| \ll |\mu|$), which is similar to the situation in the MFL theory. The real part is linear at small energies and deviates from such a dependence at $|\varepsilon| \gg |\mu|$.

The imaginary part of self-energy at finite temperature and $\varepsilon = 0$ (the inverse quasiparticle lifetime at the Fermi surface) can be obtained from the scaling arguments,

$$\gamma(T) = -[\text{Im}\Sigma(\mathbf{k}_F, \varepsilon)|_{T=0}]_{\varepsilon \rightarrow T} \quad (25)$$

Thus it is given by the same Figs. 3b, 4b, 5 with the replacement $\varepsilon \rightarrow T$ and also demonstrates the power-like behavior near the quantum phase transition.

VII. DISCUSSION AND CONCLUSIONS

In the present paper we have investigated within a scaling approach the energy dependence of the real and imaginary part of the electron self-energy in the presence of Van-Hove

singularities. We have restricted ourselves to the regions of the $\mu - T$ phase diagram, where the Fermi level is not too close to VH points (disordered ground state, $\mu_c < |\mu| \ll t$ with μ_c is the critical chemical potential) or temperature is above the critical value ($T > T_c$ with $T_c \sim \mu_c$). These regions correspond to the quantum-disordered and quantum-critical regimes in the vicinity of QPT into magnetically ordered or superconducting state.

Provided the system is not too close to QPT (at $\mu_c < |\mu| \ll t$), the imaginary part of the self-energy at VH points demonstrates in a broad energy region $|\mu| \ll |\varepsilon| \ll t$ a nearly-linear behavior, $\text{Im}\Sigma(\mathbf{k}_F, \varepsilon) \propto |\varepsilon| \ln(t/|\varepsilon|)$, which is close to that in the marginal Fermi-liquid concept [5] (however, in MFL the linear behavior of $\text{Im}\Sigma(\mathbf{k}_F, \varepsilon)$ takes place for arbitrary \mathbf{k}_F). The real part of the self-energy behaves as $\varepsilon \ln^2(t/|\varepsilon|)$. These dependences are similar to those obtained within the spin-fermion model for a nearly antiferromagnetic state [24,25], although in our case they have a different nature and are governed by Van-Hove singularities themselves rather than by closeness to antiferromagnetic quantum phase transition. The role of a characteristic spin-fluctuation frequency ω_{sf} , which separates the Fermi-liquid and MFL regimes, belongs in our case to the chemical potential $|\mu|$ ($\mu = 0$ corresponds to VH filling). Another difference is that in the presence of VH singularities the linear dependence of self-energy takes place already in the weak-coupling regime.

Near QPT, the renormalizations become important because of the large ground-state correlation length which enters renormalized vertices. Therefore the dependence $\Sigma(\mathbf{k}_F, \varepsilon)$ deviates from the nearly linear one: both real and imaginary parts of the self-energy increase considerably as $\xi_{cr}^2(T = 0)$. Such an anomalous behavior also implies a strong violation of the Fermi-liquid and even MFL picture. Within the two-patch approach, this deviation is more pronounced in the nearly-ferromagnetic state than in nearly-antiferromagnetic one (see Figs.3, 4). The reason of the distinction is that the corresponding values of t'/t , which determine the factors at the logarithmic singularities, are different. Note that the anomalies under consideration may induce the electron topological transition in the same way as discussed in Ref. [26]. The RG approach used is not able to describe the magnetically ordered or superconducting state. By this reason, the renormalized-classical regime $T < T_c$, $|\mu| < \mu_c$

should be considered within other approaches, see, e.g., Ref. [27].

In 2D situation, the physical properties near QPT should demonstrate singularities which are stronger than those in the 3D case. The correction to the electron density of states $N(\varepsilon)$ reads

$$\delta N(\varepsilon) = - \sum_{\mathbf{k}\sigma} \left[\text{Re}\Sigma(\mathbf{k},\varepsilon)\delta'(\varepsilon - \varepsilon_{\mathbf{k}}) + \frac{1}{\pi} \text{Im}\Sigma(\mathbf{k},\varepsilon)/(\varepsilon - \varepsilon_{\mathbf{k}})^2 \right] \quad (26)$$

Main contribution to the integral comes from the vicinity of VH points where the bare density of states is logarithmically divergent. Taking into account that $\text{Re}\Sigma^{(2)}(\mathbf{k},\varepsilon) \propto \varepsilon \ln^2 \max\{|\varepsilon|, |\varepsilon_{\mathbf{k}}|\}$, we obtain for the first (coherent) term in the square brackets which originates from renormalization of quasiparticle spectrum

$$\delta N_{coh}(\varepsilon) \propto \ln^3(t/|\varepsilon|), \varepsilon \gg \mu. \quad (27)$$

The calculation of the second (incoherent, non-quasiparticle) term requires the full form of $\Sigma^{(2)}(\mathbf{k},\varepsilon)$, Eq.(6), and leads to the result

$$\delta N_{incoh}(\varepsilon) \propto \ln^2(t/|\varepsilon - \mu|). \quad (28)$$

Although this divergence is slightly weaker than of the coherent term, it is not cut at $\varepsilon = \mu$. Thereby the bare VH singularity becomes considerably enhanced. Note that the divergence of the density of states together with its asymmetry in ε may lead to peculiarities of thermoelectric power owing to impurity scattering, cf. Ref. [7].

To leading (second) order the contribution to electronic specific heat owing to VH singularities has the form $\delta C \propto T \ln^3(t/ \max\{\mu, T\})$. The resistivity (inverse transport relaxation time) should demonstrate at $T > \mu$ the behavior $\rho \propto T \ln^2(t/T)$. The calculations are similar to those of Ref. [7] for the antiferromagnetic state, extra logarithmic factors coming from VH singularities. The crossover from quadratic to nearly linear temperature dependence of resistivity is confirmed by experimental data for cuprates (see, e.g., the results of Ref. [28] for the BiSrLaCuO system).

Thus the divergences in the many-electron system with VH singularities are stronger than those in the MFL theory. Near QPT, we can expect that all the physical properties

are strongly renormalized, the renormalizations being dependent on the type of the ordered phase. This problem will be considered elsewhere.

Finally we consider the application of the results obtained to cuprate systems. A nearly linear energy dependence of $\text{Im}\Sigma(\mathbf{k}_F, \varepsilon)$ at VH points, which is similar to our results (Fig.5), was observed for the system Bi2212 in ARPES experiments [29]. However, Van Hove singularities do not seem to play a decisive role in this system. As it was estimated in Refs. [24,25], for Bi2212 close to optimal doping the ratio $\omega_{sf}/|\mu|$ is about 0.1, so that the physics at not too large energies is probably determined by antiferromagnetic spin excitations rather than by critical fluctuations owing to presence of VH singularities. For the system $\text{La}_{2-x}\text{Sr}_x\text{CuO}_4$ with doping $x_c \simeq 0.2$ (which is slightly larger than optimal one) the Fermi surface crosses VH points [30]. The density of states [31], specific heat coefficient and Pauli susceptibility [32] substantially grow near this doping. The mass enhancement factor m^*/m demonstrates a similar behavior. A strong enhancement of the quasiparticle spectral weight close to the point $(\pi, 0)$ was also recently observed at $x = 0.22$ [33]. At the same time, no changes were found in the renormalization factor Z close to x_c . This may be attributed to that the critical value of μ at intermediate t'/t is very small, so that the system is still not too close to QPT induced by VH singularities. Therefore, additional experimental investigations are needed to extract a detailed form of real and imaginary parts of the self-energy near $(\pi, 0)$.

VIII. ACKNOWLEDGMENTS

We are grateful to Andrey Chubukov for useful discussions of the physical picture and experimental situation for cuprates. The research described was supported in part by Grant No.00-15-96544 from the Russian Basic Research Foundation (Support of Scientific Schools).

REFERENCES

* E-mail: Valentin.Irkhin@imp.uran.ru

- [1] P.W. Anderson, Phys.Rev.Lett. **64**, 1839 (1990); **65**, 2306 (1990); **66**, 3326 (1991); **71**, 1220 (1993); *The Theory of Superconductivity in High- T_c Cuprates*, Princeton University Press, Princeton, N.Y., 1997.
- [2] P.Bloom, Phys.Rev.B**12**, 125 (1975).
- [3] H.Fukuyama and Y.Hasegawa, Progr. Theor. Phys. Suppl. **101**, 441 (1990).
- [4] C.Hodges, H.Smith and J.W.Wilkins, Phys.Rev.B**4**, 302 (1971).
- [5] C. M. Varma, P. B. Littlewood, S. Schmitt-Rink, E. Abrahams, and A. E. Ruckenstein, Phys. Rev.Lett. **63**, 1996 (1989), **64**, 497 (1990).
- [6] T.Moriya, Y.Takahashi, and K.Ueda, J.Phys.Soc.Jpn **59**, 2905 (1990).
- [7] V.Yu. Irkhin and M.I. Katsnelson, Phys.Rev.B**52**, 6181 (1995); Phys. Rev.B**62**, 5647 (2000).
- [8] P.C.Pattnaik et al, Phys.Rev.B**45**, 5714 (1992); D.M. Newns et al, Phys.Rev.B**52**, 13611 (1995); S.Gopalan, O.Gunnarson and O.K.Andersen, Phys.Rev.B**46**, 11798 (1992).
- [9] V.Yu. Irkhin, A.A. Katanin, and M.I. Katsnelson, Phys. Rev.B, in press; cond-mat/0102381.
- [10] M.Salmhofer and C.Honerkamp, cond-mat/0105218.
- [11] I. E. Dzyaloshinskii, J.Phys.I (France) **6**, 119 (1996).
- [12] D. Menashe and B. Laikhtman, Phys.Rev.B **59**, 13592 (1999).
- [13] J.Kishine, N.Furukawa and K.Yonemitsu, Phys. Rev.B**59**, 14823 (1999).
- [14] C.Honerkamp, cond-mat/0103172.

- [15] A.J.Millis, Phys. Rev.B**48**, 7183 (1993).
- [16] S.Sachdev, *Quantum Phase Transitions*, Cambrige University Press, Cambrige, 1999.
- [17] J.Gonzalez, F.Guinea and M.A.H.Vozmediano, Nucl.Phys. B, **485**, 694 (1997).
- [18] P. Lederer, G. Montambaux, and D. Poilblanc, J. Phys. (Paris) **48**, 1613 (1987).
- [19] N. Furukawa, T. M. Rice, and M. Salmhofer, Phys. Rev. Lett. **81**, 3195 (1998).
- [20] J. Solyom, Adv. Phys. **28**, 201 (1979).
- [21] C. Bourbonnais and L. Caron, Int. J. Mod. Phys.B**5**, 1033 (1991).
- [22] N. Dupuis and G.Chitov, Phys. Rev. B**54**, 3040 (1996); N. Dupuis, Eur. Phys. J B**3**, 315 (1998); cond-mat/9604189.
- [23] C. Honerkamp, M. Salmhofer, N. Furukawa, and T. M. Rice, Phys. Rev. B**63**, 35109 (2001).
- [24] A. Chubukov, Phys.Rev.B**52** R4837 (1995); Europhys. Lett.**44**, 655 (1998); A.Chubukov and J.Schmalian, Phys. Rev. B**57**, R11085 (1998).
- [25] A. Abanov, A.V. Chubukov and J.Schmalian, to be published.
- [26] A.V. Chubukov, D.K. Morr and K.A. Shakhnovich, Phil. Mag. B**74**, 563 (1996).
- [27] Y.M. Vilk et al, J.Phys.I (France), **7**, 1309 (1997).
- [28] S. Ono, Y. Ando, G.S. Boebinger et al, Phys. Rev. Lett. **85**, 638 (2000).
- [29] T. Valla et al, Science **285**, 2110 (1999); Phys. Rev. Lett. **85**, 828 (2000).
- [30] A.Ino et. al., cond-mat/0005370
- [31] A. Ino et al, Phys. Rev. Lett. **81**, 2124 (1998)
- [32] N. Momono et al, Physica C**233**, 395 (1994); T.Nakano et al, Phys.Rev.B**49**, 16000 (1994).

FIGURES

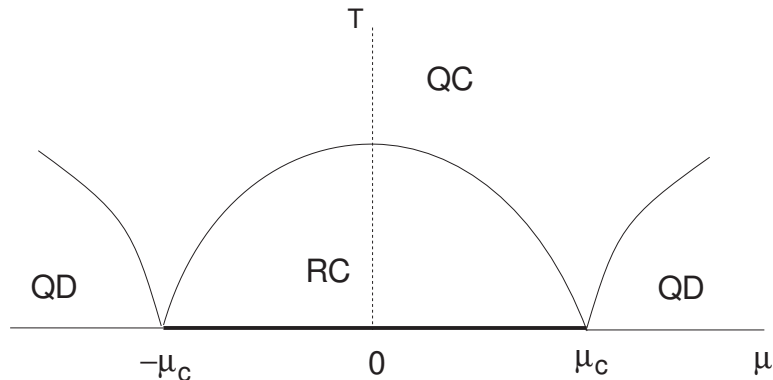


Fig.1. A qualitative $T - \mu$ phase diagram in the vicinity of the quantum phase transition.

The chemical potential μ is referred to the Van Hove singularity. Bold line denotes the ordered ground state.

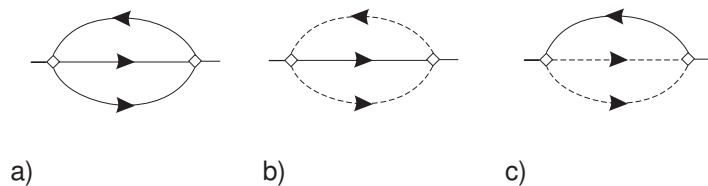
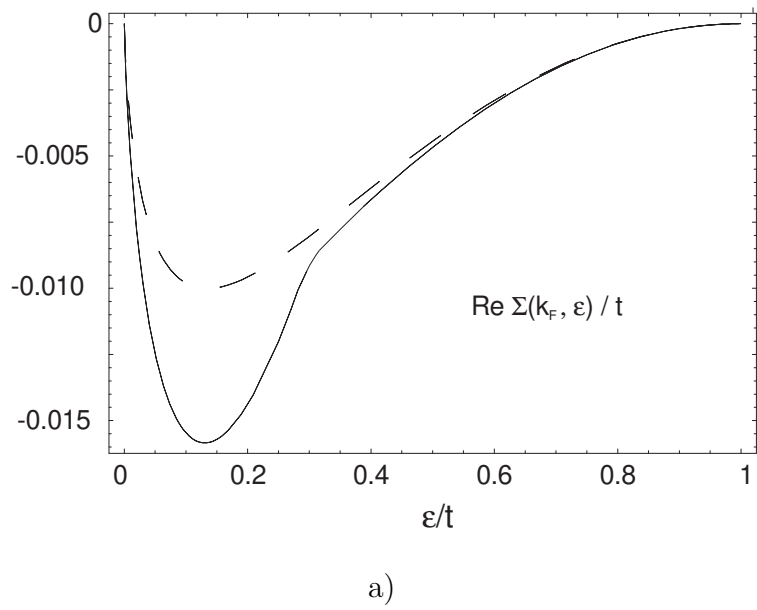
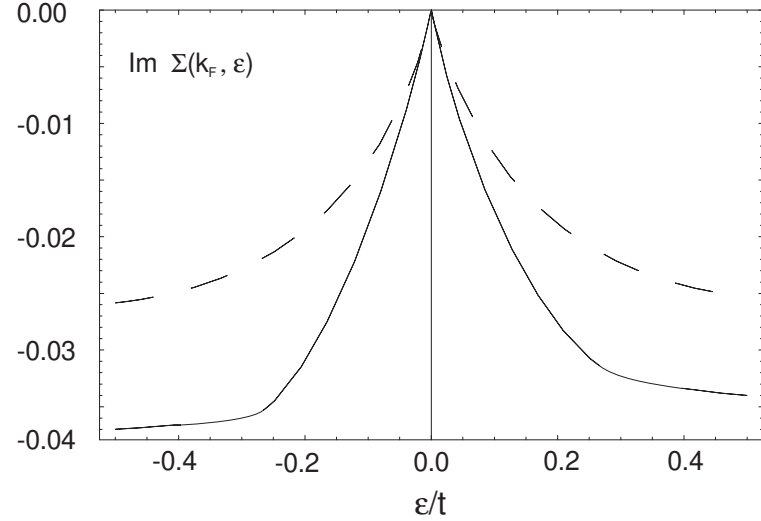
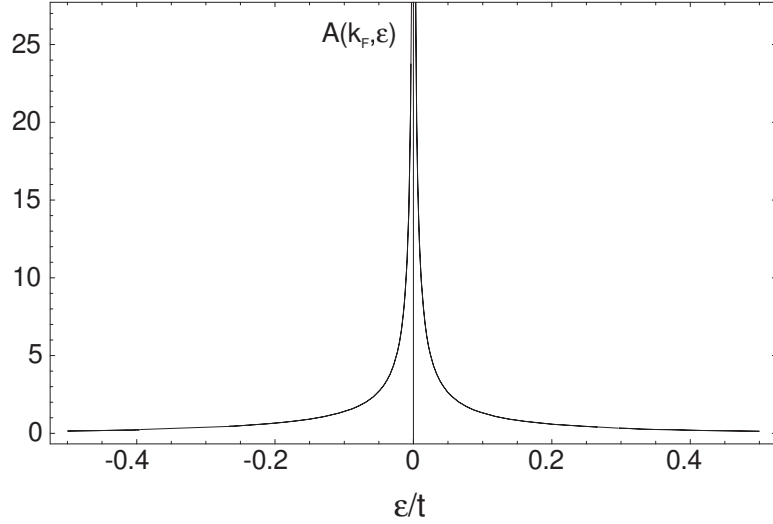


Fig.2. The second-order diagrams for the electron self-energy. Solid and dashed lines correspond to electrons with momenta close to $(0, \pi)$ and $(\pi, 0)$ Van-Hove singularities respectively



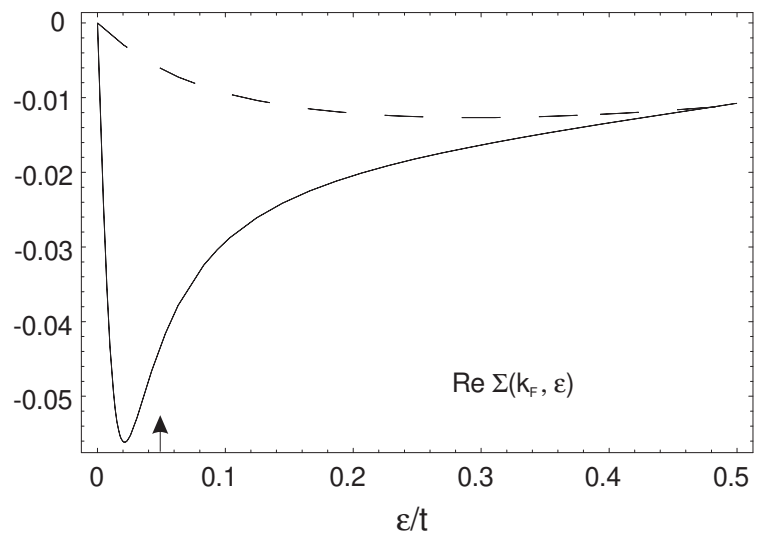


b)

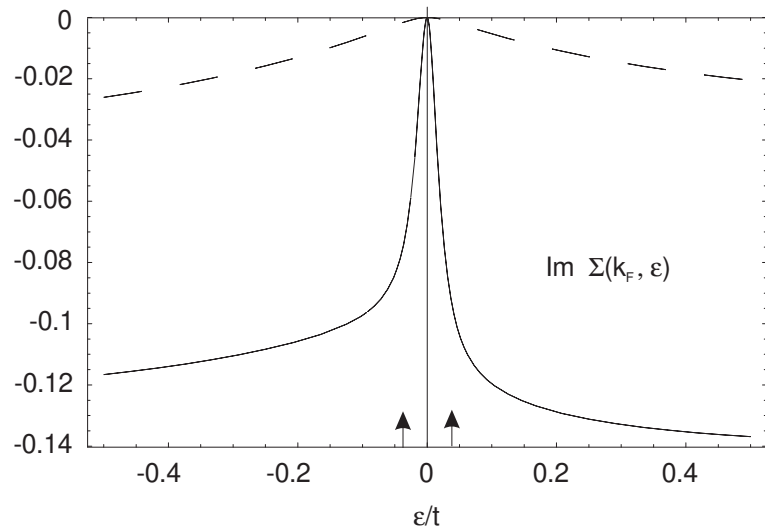


c)

Fig.3. The energy dependences of real (a) and imaginary (b) parts of the self-energy at VH points, and the spectral weight (c) for $t'/t = -0.15$, $U = 4t$, $\mu/t = 2 \cdot 10^{-4}$ and $T = 0$. The dashed line corresponds to the second-order perturbation result.



a)



b)

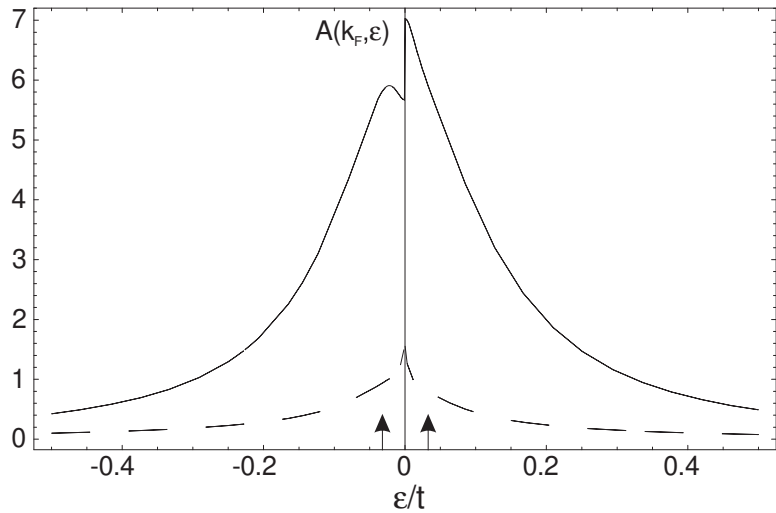


Fig.4. The energy dependences of real (a) and imaginary (b) parts of the self-energy at VH points, and the spectral weight (c) for $t'/t = -0.45$, $U = 4t$, $\mu/t = 0.045$ and $T = 0$. The dashed line corresponds to the second-order perturbation result. The arrows mark the chemical potential.

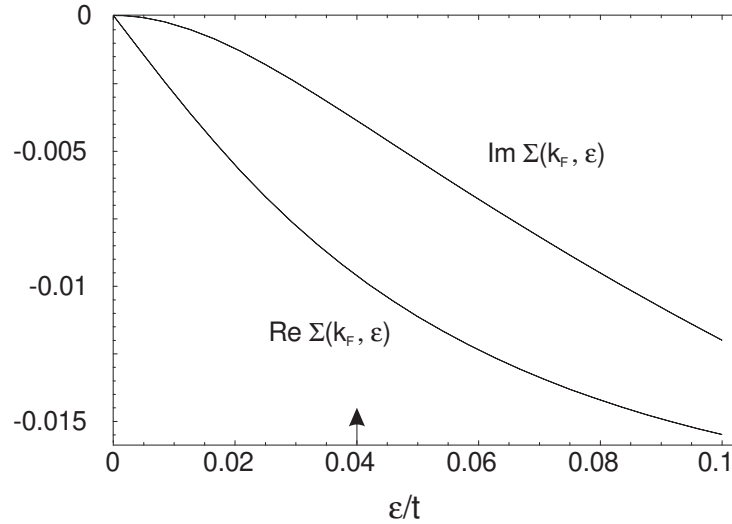


Fig.5. The energy dependences of real and imaginary parts of the self-energy for $t'/t = -0.30$, $U = 4t$, $\mu/t = 0.04$ and $T = 0$. The arrow marks the chemical potential.